Send Orders for Reprints to reprints@benthamscience.ae

The Open Mechanical Engineering Journal, **2015,** *9,* **1057-1061**

Open Access

Dynamic Responses of Rotor Drops onto Auxiliary Bearing with the Support of Metal Rubber Ring

Zhu Yili* and Zhang Yongchun

Department of Electrical Engineering, Changzhou Institute of Technology, Changzhou, Jiangsu, 213002, P.R. China

Abstract: In an active magnetic bearing (AMB) system, the Auxiliary bearings (ABs) are indispensable to protect the rotor and stator in case of AMB failure. Most of the former researches try to modify relevant design parameters of ABs to buffer the following impacts and heating after rotor drop. Based on the analysis of the disadvantages of traditional ABs, a new type of AB with the support of metal rubber ring is proposed to enhance the AB work performance in AMB system. Detailed simulation models containing rigid rotor model, contact model between rotor and inner race as well as AB system model after rotor drop are established. Then, using those established models the dynamic responses are simulated to obtain proper metal rubber ring support characteristics. Finally, relevant rotor drop experiments are carried out on the established AMB test bench. The experiment results verify the advantages of the new type ABs and the correctness of simulation analysis.

Keywords: Active magnetic bearing, auxiliary bearing, dynamic response, metal rubber ring, rotor drop.

1. INTRODUCTION

Active magnetic bearings (AMBs) have many advantages over conventional mechanical bearings, such as no mechanical friction and lubrication, adjusted support stiffness and damping. However, the ABs are indispensable to protect the AMB assembly after a possible AMB failure.

Most of the former researches have focused on the dynamic responses after rotor drop. Kirk *et al*. [1, 2] studied the influences of the support stiffness and damping by evaluating dynamic response for various rotor-support system parameters. They showed an optimum damping can be selected to prevent destructive backward whirl. Fumagalli *et al.* [3] classified the rotor drop process into four distinct motion phases: free fall; impact; sliding; and rolling. Sun [4] conducted numerical simulations of a rotor drop onto the AB in flywheel energy storage system using a detailed AB model which includes a Hertzian load-deflection relationship between mechanical contacts, speed-and-preload-dependent bearing stiffness due to centrifugal force, and a drag friction torque. Xie and Flowers [5] numerically investigated the steady-state behavior of a rotor drops onto ABs and primarily looked at the effects of various parametric configurations: rotor imbalance, support stiffness and damping. Foiles and Allaire [6] also numerically analyzed the effects of parameters for non-linear models on two types of rotors: generator or turbine rotor and centrifugal compressor rotor. Cole *et al*. [7] developed a deep groove AB model considering the elastic deformation of the inner race, mainly studied the impact force and effects of bearing width as well as ball load distributions. Kaur [8] tested the performances of powder lubricated bearings used as AB.

However, most of those researches focused on the relevant parameters of AB itself. For it is hard to modify the bearing stiffness and damping to satisfy the optimum simulation results, a new type CB with the support of metal rubber ring is proposed in this paper. Because of the excellent buffer characteristics of metal rubber ring, it can to some extent buffer rotor vibrations after rotor drop. The performances of the new type AB are analyzed by both simulations and experiments.

2. SIMULATION

2.1. Structure of AMB System

Fig. (**1**) shows the studied structure of a motor drive system equipped with magnetic bearings, where 1: rotor; 2: radial displacement sensor; 3: axial displacement sensor; 4: auxiliary bearing; 5: axial magnetic bearing; 6: radial magnetic bearing; 7-motor. The motor is located between the

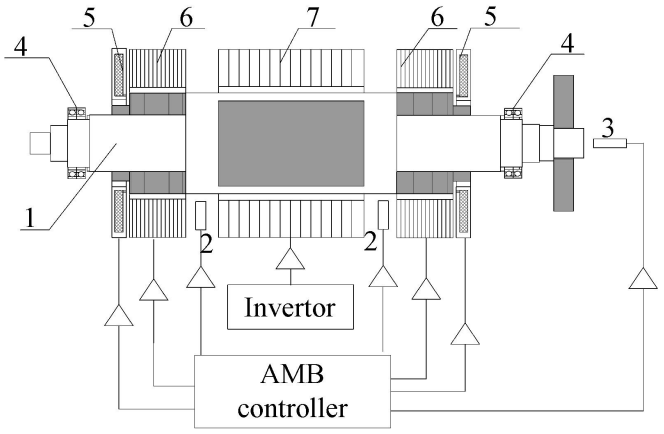

Fig. (1). Structure of AMB System.

1874-155X/15 2015 Bentham Open

two radial magnetic bearings. Each radial magnetic bearing generates radial forces. Axial magnetic bearings regulate the axial forces in the shaft direction. Besides those magnetic bearings, two auxiliary bearings are located in the two ends of the structure respectively to prevent damages after rotor drop. The air gap between the auxiliary bearing inner race and the rotor is half of the air gap of AMB.

The two types of AB are presented in Fig. (**2**). Compared with traditional AB, a metal rubber ring is installed in the new type AB.

(**a**) Traditional auxiliary bearing

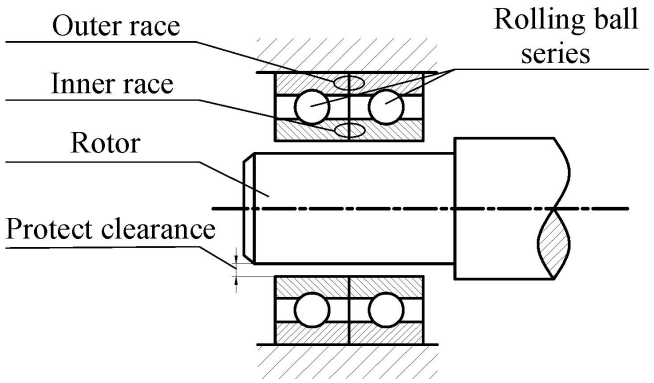

(**b**) New type auxiliary bearing

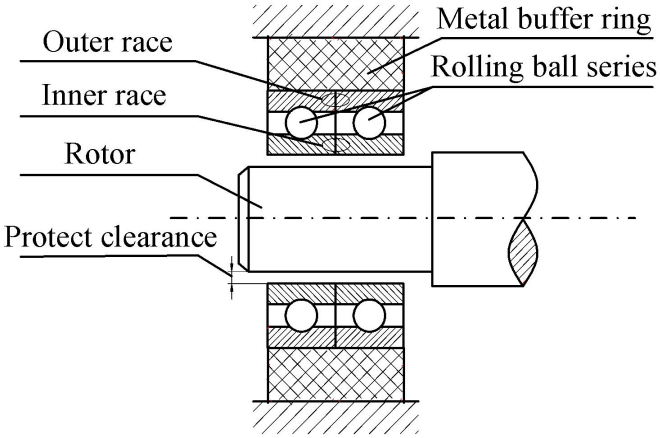

Fig. (2). Structure of analyzed auxiliary bearing.

2.2. Simulation Model

According to the structure of AMB system, the rotor force model can be obtained, as shown in Fig. (**3**). When the AMB system is in normal operation, the rotor bears left-hand and right-hand magnetic bearing forces (F_{a1x}, F_{a1y} and F_{a2x}, F_{a2y}), centrifugal forces (F_{cx}, F_{cy}) and gravity (G_r) respectively. After AMB system failure, the rotor bears left-hand and right-hand AB forces (F_{b1x}, F_{b1y} and F_{b2x}, F_{b2y}), centrifugal forces (F_{cx}, F_{cy}) and gravity (G_r) respectively.

Then the rotor motion equation can be written as:

$$\mathrm{m}\ddot{\mathrm{x}} + \mathrm{G}\dot{\mathrm{x}} = \mathrm{A}\mathrm{F}_a + \mathrm{B}\mathrm{F}_b + \mathrm{F}_c + \mathrm{F}_g \tag{1}$$

where mass matrix $\mathrm{m} = \mathrm{diag}\left(m_r, m_r, J, J\right)$, m_r is rotor mass, J is rotor transverse moment of inertia (MOI), barycenter displacement $\mathrm{x} = \left(x_r, y_r, \theta_x, \theta_y\right)^{\mathrm{T}}$, x_r and y_r are the displacements of barycenter in the direction of x and y axis respectively, θ_x and θ_y are the rotational displacement of barycenter around the direction of x and y axis respectively. G is the gyroscopic torque matrix,

$$\mathrm{G} = \begin{pmatrix} 0 & 0 & 0 & 0 \\ 0 & 0 & 0 & 0 \\ 0 & 0 & 0 & \omega J_z \\ 0 & 0 & -\omega J_z & 0 \end{pmatrix},$$

J_z is rotor polar MOI, ω is the rotor angular velocity. A and B are the introduced coefficient matrixes,

$$\mathrm{A} = \begin{pmatrix} 1 & 0 & 1 & 0 \\ 0 & 1 & 0 & 1 \\ 0 & l_{a1} & 0 & -l_{a2} \\ -l_{a1} & 0 & l_{a2} & 0 \end{pmatrix}, \ \mathrm{B} = \begin{pmatrix} 1 & 0 & 1 & 0 \\ 0 & 1 & 0 & 1 \\ 0 & l_{b1} & 0 & -l_{b2} \\ -l_{b1} & 0 & l_{b2} & 0 \end{pmatrix};$$

magnetic force vector $\mathrm{F}_a = \left(F_{a1x}, F_{a1y}, F_{a2x}, F_{a2y}\right)^{\mathrm{T}}$; rotor centrifugal force vector $\mathrm{F}_a = \left(F_{cx}, F_{cy}, 0, 0\right)^{\mathrm{T}}$; rotor gravity vector $\mathrm{F}_g = \left(F_{gx}, F_{gy}, 0, 0\right)^{\mathrm{T}}$.

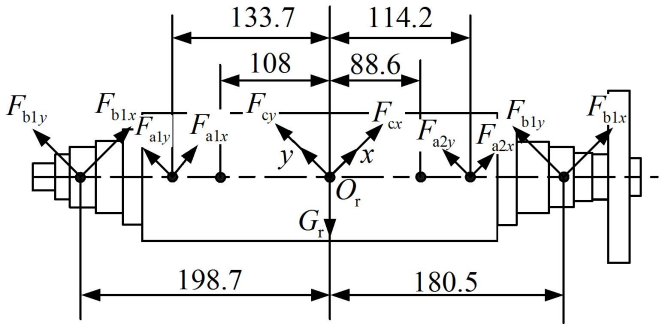

Fig. (3). Rotor force model.

The contact model after rotor drops onto the AB supported by metal rubber ring is shown in Fig. (**4**). Here the model of metal rubber ring is seemed as stiffness K_{rr} and damping C_{rr}, which is installed between the bearing house and foundation support. F_n and F_t are the normal impact force and tangential frictional force between the rotor and inner race, respectively; R_r and R_b are the shaft radius and inner race bore radius at the AB position, respectively; m_i is the mass of the inner race, and the bearing outer race is rigidly installed in the bearing house, the whole mass is m_o; C_b and C_{rr} are the support damping of the bearing and metal rubber ring, respectively; x_b and x_i are the vibration displacements of the rotor and inner race in the x-axis, respectively; y_b and y_i are the vibration displacements of the rotor and inner race in the y-axis, respectively; ϕ_i is the defined rotor-inner race contact angle, and $\sin\phi_i = \left(y_i - y_o\right)/u_i$, $\cos\phi_i = \left(x_i - x_o\right)/u_i$, where $u_i = \sqrt{\left(x_i - x_o\right)^2 + \left(y_i - y_o\right)^2}$, To simplify the analysis, it is assumed that there always exists a ball labeled as "1" in the direction of relative displacement

between the inner and outer race, so the *j*th ball position angle moving counterclockwise is $\varphi_j = 2\pi(j-1)/N_b$, where N_b is the ball number of the single bearing. In the same way, θ_r and θ_i are the angular displacements of the rotor and inner race respectively, and δ_b is the penetration depth between the rotor and inner race.

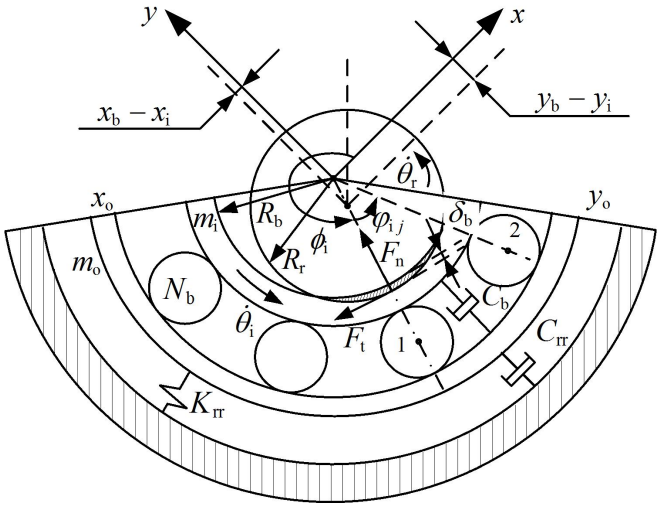

Fig. (4). Contact model after rotor drop.

The radial motion equation for the new type AB inner race and bearing house after rotor drop is given by

$$\mathrm{M_b}\ddot{\mathrm{x}}_b + \mathrm{C_b}\dot{\mathrm{x}}_b = \mathrm{F_b} + \mathrm{F_{rb}} \tag{2}$$

where the mass matrix $\mathrm{M_b} = \mathrm{diag}(m_i, m_i, m_o, m_o)$; the forces from the balls and metal rubber ring $\mathrm{F_b} = \left(F_{ix}, F_{iy}, F_{ex} + F_{rx}, F_{ey} + F_{ry}\right)^{\mathrm{T}}$; the vibration displacement vector $\mathrm{x_b} = \left(x_i, y_i, x_o, y_o\right)^{\mathrm{T}}$; the forces from the rotor $\mathrm{F_{rb}} = \left(F_{bx}, F_{by}, 0, 0\right)^{\mathrm{T}}$; the damping matrix

$$\mathrm{C_b} = \begin{bmatrix} 2C_b & 0 & -2C_b & 0 \\ 0 & 2C_b & 0 & -2C_b \\ -2C_b & 0 & 2C_b + C_{rr} & 0 \\ 0 & -2C_b & 0 & 2C_b + C_{rr} \end{bmatrix}.$$

The rotational equation of the inner race can be written as:

$$J_z\ddot{\theta}_i = F_t R_b - 2T_i \tag{3}$$

where T_i is the internal friction moment of the bearing.

2.3. Simulation Results

The whole simulation composes two parts, rotor motions before and after AMB failure. Firstly, the rotor motions during normal operation are simulated as the initial conditions for the dynamic simulations after rotor drop. During the simulation, based on relevant AMB theory, hertz contact theory and well as ball bearing support theory [9], the AMB forces and AB forces are calculated using the real time rotor and AB motions. The chosen ball bearing type is 61905, and some other simulation parameters are listed in Table **1**.

Table 1. Relevant simulation parameters.

Parameter	Value
Rotor unbalance e_r (μm)	2.5
Rotor transverse MOI J (kg·mm^2)	6.1e5
Rotor polar MOI J_z (kg·mm2)	4.7e3
Mass of the inner race m_i (kg)	16.4e-3
Mass of the bearing house m_o (kg)	0.35
Current stiffness of AMB k_i (N/A)	166.5
Displacement stiffness of AMB k_x (N/m)	1.25e6
Protective gap of ABs c_{r1} (mm)	0.125
Mass of rotor m_r kg	9.1

The maximum impact forces between rotor and inner race after rotor drop for different metal rubber ring support stiffness and damping at the initial rotor rotational speed 12 000 r/min, 18 000 r/min, 24 000 r/min and 30 000 r/min can be calculated after obtaining the rotor and AB motions by simulation. The results are presented in Fig. (**5**). According to the simulation results, it can be seen that choosing support stiffness 1e6 N/m and support damping 1e4 N.s/m are advisable to buffer the following impact forces after rotor drop.

3. EXPERIMENTS

Providing the above obtained support stiffness and damping, the metal rubber ring is manufactured by professional factory. Fig. (**6**) shows the part installed the metal rubber ring. Fig. (**7**) presents the rotor drop test rig, where 1:PC; 2: AMB system controller; 3: high-speed magnetic levitation motor; 4: inverter; 5: Labview data acquisition (DAQ) boards; 6: software of data acquisition system. The displacement sensor signals are collected by Labview DAQ boards and saved in the PC. A subsequent analysis of the collected data is carried out using MATLAB software.

Using the collected displacement sensor signals, the rotor orbits 0.1 s before rotor drop and 0.2 s after rotor drop onto different types of AB at the initial rotor speed 12 000 r/min can be obtained, as shown in Fig. (**8**). It is obviously that the use of metal rubber ring can effectively reduce the vibrations after rotor drop.

Once the rotor vibrations after rotor drop are obtained by the experiments, using equation (1) the support forces of ABs can be calculated as:

$$\mathrm{F_b} = \mathrm{inv}(\mathrm{m}\ddot{\mathrm{x}} + \mathrm{G}\dot{\mathrm{x}} - \mathrm{F_c} - \mathrm{F_g}) \tag{4}$$

The maximum impact forces calculated using the experimental results 0.5 s after rotor drops are shown in Fig. (**9**). The results indicate that the proposed new type AB can effectively reduce the impact forces after rotor drop.

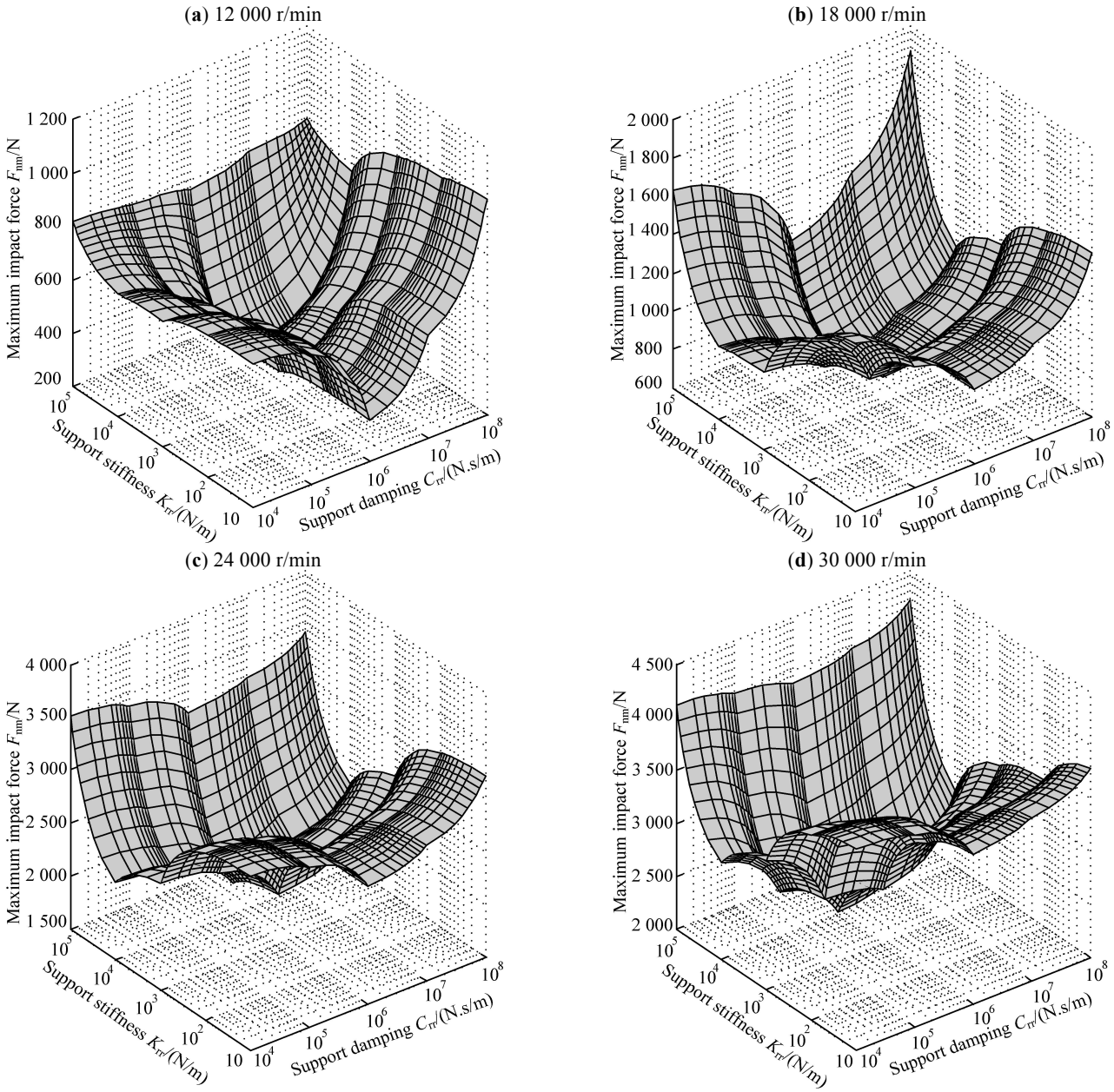

Fig. (5). Influences of metal rubber ring support characteristics on maximum impact forces.

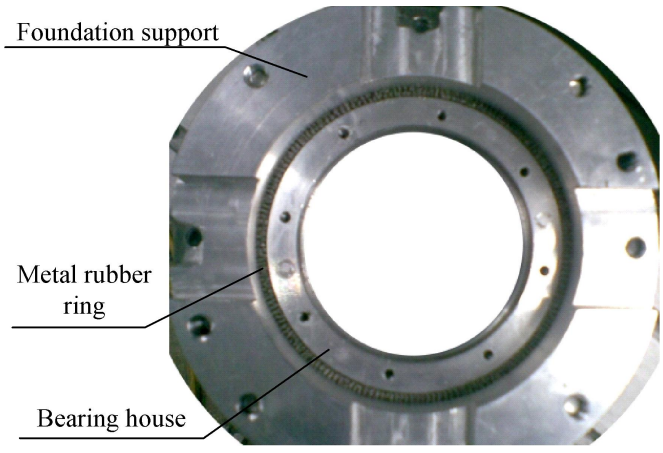

Fig. (6). Photograph of new type AB block.

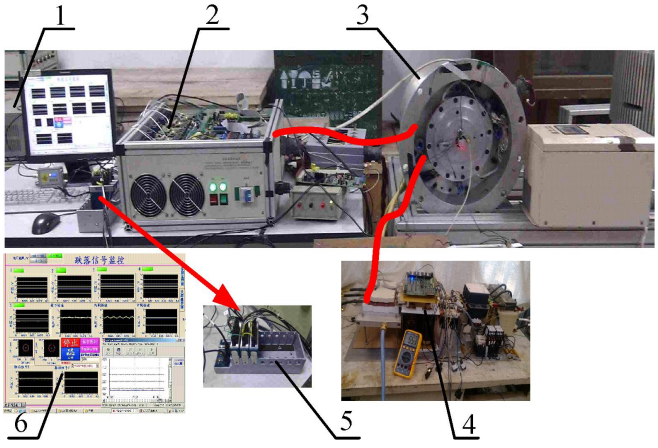

Fig. (7). Rotor drop experiment rig.

(**a**) Traditional AB

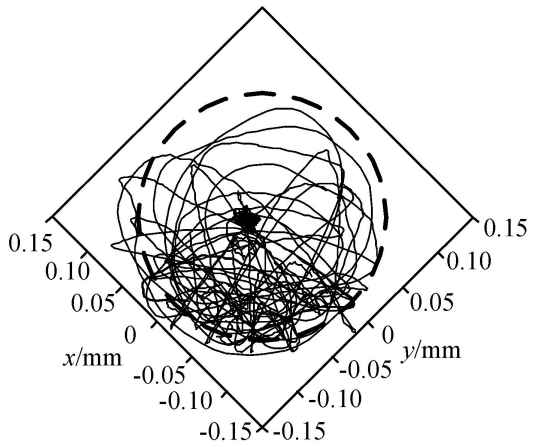

(**b**) New type AB

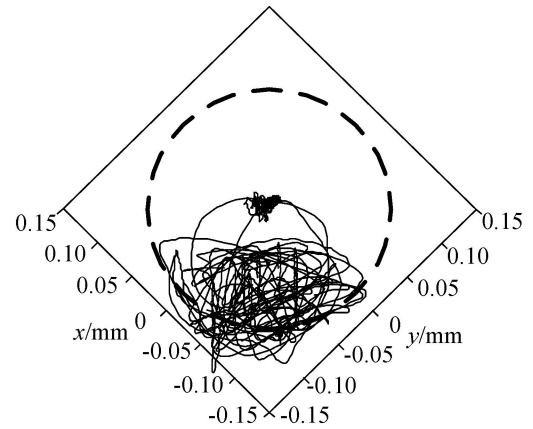

Fig. (8). Rotor orbits obtained by experiments.

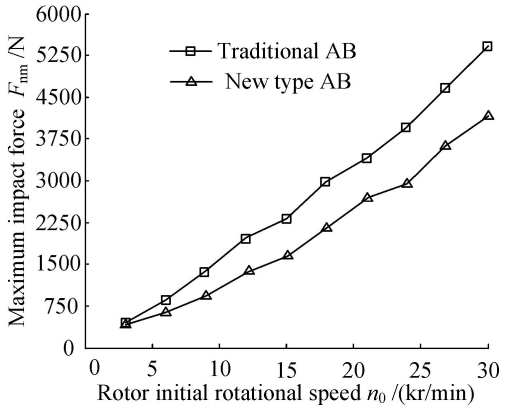

Fig. (9). Maximum impact force obtained by experiments.

CONCLUSION

In this paper, the new type AB with metal rubber ring is proposed to improve the working performances of AB in AMB system. The relevant dynamic responses after AMB failure are theoretically simulated and experimentally verified. The following conclusions can be obtained from the above researches.

1) It is necessary to establish dynamic models to obtain proper support characteristics of metal rubber ring before manufacture.

2) Use of proper metal rubber ring helps to reduce the rotor vibration amplitudes and impact forces after rotor drop.

CONFLICT OF INTEREST

The authors confirm that this article content has no conflict of interest.

ACKNOWLEDGEMENTS

This work was financially supported by National Natural Science Foundation of China (51405040); the Applied Basic Research in Chanzhou city of China (CJ20140048).

REFERENCES

[1] T. Ishii, and R. G. Kirk, "Transient response technique applied to active magnetic bearing machinery during rotor drop," *Journal of Rotating Machinery and Vehicle Dynamics*, vol. 35, pp. 191-199, 1991.

[2] R. G. Kirk, and T. Ishii, "Transient rotor drop analysis of rotor following magnetic bearing power outage," In: *Proceedings of MAG '93 Magnetic Bearings, Magnetic Drives, and Dry Gas Seals Conference & Exhibition,* Alexandria, VA, USA, 1993, pp. 53-61.

[3] M. Fumagalli, P. Varadi, and G. Schweitzer, "Impact dynamics of high speed rotors in retainer bearings and measurement concepts," In: *Proceedings of 4th International Symposium on Magnetic Bearings,* Zurich, Switzerland, pp. 239-244, 1994.

[4] G. Sun, A. B. Palazzolo, A. Provenza, and G. Montague, "Detailed ball bearing model for magnetic suspension auxiliary service," *Journal of Sound and Vibration*, vol. 269, pp. 933-963, 2004.

[5] H. Xie, and G. T. Flowers, "Steady-state dynamic behavior of an auxiliary bearing supported rotor system," In: *Proceedings of American Society of Mechanical Engineers Winter Annual Meeting*, Chicago, USA, 1994, pp. 1-11.

[6] W. C. Foiles, and P. E. Allaire, "Nonlinear transient modeling of active magnetic bearing rotors during rotor drop on auxiliary bearing," In: *Proceedings of MAG ' 97 Industrial Conference and Exhibition on Magnetic Bearings*, Alexandria, VA, USA, 1997, pp. 154-163.

[7] M. O. T. Cole, P. S. Keogh, and C. R. Burrows, "The dynamic behavior of a rolling element auxiliary bearing following rotor impact", *Journal of Tribology*, vol. 124, pp. 406-606, 2002.

[8] R. G. Kaur, and H. Heshmat, "100 mm diameter self-contained solid/powder lubricated auxiliary bearing operated at 30, 000 rpm ", *Tribology Transactions*, vol. 45, no. 1, pp. 76-84, 2002.

[9] T. A. Harris, *Rolling Bearing Analysis,* 3rd ed. John Wiley & Sons Ltd, 1991, pp. 15-45.

Received: February 17, 2014 Revised: March 21, 2015 Accepted: June 9, 2015